JETIR.ORG ISSN: 2349-5162 | ESTD Year : 2014 | Monthly Issue
JOURNAL OF EMERGING TECHNOLOGIES AND INNOVATIVE RESEARCH (JETIR)
An International Scholarly Open Access, Peer-reviewed, Refereed Journal

ENERGY MANAGEMENT SYSTEM FOR HYBRID ELECTRICAL VEHICLE USING A BIDIRECTIONAL DC/DC CONVERTER USING FUZZY LOGIC CONTROLLER

PALIKELA RAMACHANDRA MURTHY[1] U P KUMAR CHATURVEDULA[2] K MANOZ KUMAR REDDY[3]

M.Tech Student, Department of EEE, Aditya College of Engineering, ,Surampalem ,AP, India.1
Associate Professor, Department of EEE, Aditya College of Engineering, ,Surampalem ,AP, India.2
Associate Professor, Department of EEE, Aditya College of Engineering, ,Surampalem ,AP, India.3

ABSTRACT

This project organizes a application of hybrid electric vehicle systems operated with novel designed bidirectional dc-dc converter (BDC) which interfaces a main energy storage (ES1),an auxiliary energy storage (ES2) and dc bus of different voltage levels. Proposed BDC converter can operate both step up and step down mode. In which step up mode represents low voltage dual source -powering mode and step down mode represents high voltage dc link energy – regenerating mode, both the modes are operated under the control of bidirectional power flow. This model can independently control power flow between low voltage dual source buck/boost modes. Here in, the circuit configuration, operation, steady-state analysis, and closed-loop control of the proposed BDC are discussed according to its three modes of power transfer. In this project fuzzy logic controller is used and also system results are validates through **MATLAB/SIMULINK** software.

Index Terms—Bidirectional dc/dc converter (BDC), dual battery storage, hybrid electric vehicle, Fuzzy logic controller.

I. INTRODUCTION

Worldwide environmental change and energy supply is declining have stimulated changes in vehicular innovation. For the applications in future vehicles the advanced technologies are currently being investigated. Among such applications, fuel-cell hybrid electric vehicles (FCV/HEV) are efficient and promising candidates. Before, Ehsani et al. studied the vehicles' dynamics to look for an optimal torque-speed profile of the electric propulsion

system [1]. Emadi et al. talked about the working properties of the geographies for
various vehicles including HEV, FCV, and more electric vehicles [2]. To satisfy huge vehicular load, for advanced vehicular power system Emadi et al. also integrated power electronics intensive solutions [3]. Schaltz et al. sufficiently divide the load power among the fuel cell stack, the battery, and the ultra capacitors based on two proposed energy-management strategies [4]. Thounthong et al.studied the impact of fuel-cell (FC) execution and the benefits of hybridization for control systems [5]. Chan et al. reviewed electric, hybrid, and fuel-cell vehicles and concentrated on structures and modeling for energy management [6]. Khaligh and Li introduced energy-storage topologies for HEVs and plug-in HEVs (PHEVs).

They also analysed and compared battery, UC, and FC technologies. Moreover, they also addressed various hybrid ESSs that integrate two or more storage devices [7]. Rajashekara talked about the flow status and the necessities of essential electric drive parts-the battery, the electric motors, and the power electronics system [8]. Lai et al. implemented a bidirectional dc/dc converter topology with two-stage and interleaved qualities.

The Voltage Transformation ratio of the converter has improved in the EV and DC micro grid systems. In addition, Lai also examined a bidirectional dc to dc converter (BDC) topology which has a high voltage transformation ratio for EV batteries associated with a dc-micro grid system [10]. In FCV systems, the primary battery storage device is commonly used to begin the FC and to supply power to the propulsion motor [2, 3].

The battery storage devices improve the inherently slow response time for the FC stack through supplying peak power during accelerating the vehicle [7]. Besides, it contains a high power-density component for example, super capacitors (SCs) eliminate peak power transients during accelerating and regenerative braking [11]. In general, SCs can store regenerative energy during deceleration and release it during acceleration, thereby supplying additional power. The high power density of SCs prolongs the life span of both FC stack and battery storage devices and improves the overall efficiency of FCV systems.

This investigation proposes an interleaved voltage-doublers structure [9, 28] and a synchronous buck-boost circuit are a two new BDC topologies for FCV/HEV power system. It highlights two essential working modes: a low-voltage double-source-powering mode and a high-voltage dc-bus energy-regenerating mode. In addition when the converter is in low-voltage dual-source buck-boost mode the proposed converter can independently control power flow between any two low-voltage sources. A similar topology was presented in [29] that just discuss a short idea. On the other hand, this investigation presents detailed analysis of the operation and closed-loop control of this new topology as well as simulation results for all its modes of operation. The proposed converter can operate over a wider range of voltage levels that's why this study expanded the topology presented in [29].

The principle attributes of the proposed converter are summed up as follows:

- Interfaces more than two dc sources for various voltage levels,
- Controls power flow between the dc bus and the two low-voltage sources and furthermore independently controls power flow between the two low-voltage sources,
- Enhances static voltage gain and therefore decreases switch voltage stress, and
- Possesses a sensible duty cycle and makes a wide voltage distinction between its high-and low-side ports.

A functional diagram for a typical (FCV/HEV) power system is illustrated in Fig. 1 [4, 13]. The low-voltage FC stack is used as the main power source, and SCs directly connected in parallel with FCs. The dc/dc power converter is used to convert the FC stack voltage into a sufficient dc-bus voltage in the driving inverter for supplying power to the propulsion motor. Furthermore, ES1 with rather higher voltage is used as the main battery storage device for supplying peak power, and ES2 with rather lower voltage could be an auxiliary battery storage device to achieve the vehicle range extender concept [13]. The function of the bidirectional dc/dc converter (BDC) is to interface dual-battery energy storage with the dc-bus of the driving inverter. Generally, the FC stack and battery storage devices have different voltage levels. Several multiport BDCs have been developed to provide specific voltages for loads and control power flow between different sources, thus reducing overall cost, mass, and power consumption [14-27]. These BDCs can be categorized into isolated and non isolated types.

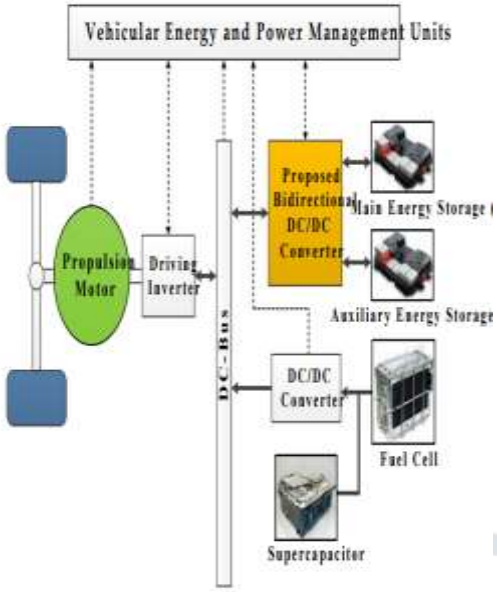

Fig.1.Typical functional diagram for a FCV/HEV power system.

In isolated converters, high-frequency power transformers are applied to enable galvanic isolation. A few isolated multiport BDC topologies have been investigated, such as the fly back, half- or full-bridge circuits, dual-active bridges, and resonant circuits . The literature suggests that non isolated BDCs are more effective than typical isolated BDCs in EVs .Liu et al. derived non isolated multi-input converter topologies by way of a combination of buck, boost, Ćuk, and Sepic. In [23], Wu et al. developed the three-port non isolated multi-input-multi-output (MIMO) converter topologies for interfacing a renewable source, a storage battery, and a load simultaneously. The three double-input converters developed in [19] comprise a single-pole triple-throw switch and only one inductor. A modular non isolated MIMO converter was presented . This converter is applied to hybridize clean energy sources of EVs and the basic boost circuit was modified and integrated. However, the voltage gain of the MIMO boost circuit is limited in practice, because of the losses associated with some components such as the main power switch, inductor, filter capacitor, and rectifier diode.

To overcome this drawback, three-port power converter that has high-gain characteristic and contains FC, battery sources and stacked output for interfacing HEV, as well as a dc-micro grid was presented. Although the multiport BDC discussed,can interface more than two sources of power and operate at different voltage levels, it still has limited static voltage gains, resulting in a narrow voltage range and a low voltage difference between the high and low-side ports.

II. PROPOSED TOPOLOGY

The proposed BDC topology with dual-battery energy storage is illustrated in Fig.1, where VH, VES1, and VES2 represent the high-voltage dc-bus voltage, the main energy storage (ES1), and the auxiliary energy storage (ES2) of the system, respectively. Two bidirectional power switches (SES1 and SES2) in the converter structure, are used to switch on or switch off the current loops of ES1 and ES2, respectively. A charge-pump capacitor (CB) is integrated as a voltage divider with four active switches (Q1, Q2, Q3, Q4) and two phase inductors (L1, L2) to improve the static voltage gain between the two low-voltage dual sources (VES1, VES2) and the high-voltage dc bus (VH) in the proposed converter. Furthermore, the additional CB reduces the switch voltage stress of active switches and eliminates the need to operate at an extreme duty ratio. Furthermore, the three bidirectional power switches (S, SES1, SES2) displayed in Fig. 2 exhibit four-quadrant operation and are adopted to control the power flow between two low-voltage dual sources (VES1, VES2) and to block either positive or negative voltage.

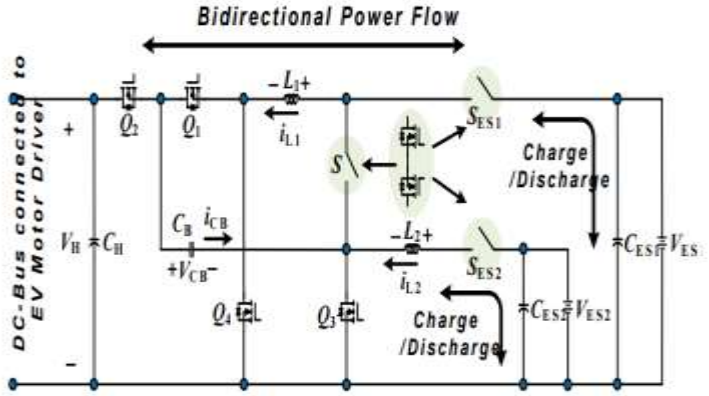

Fig.2.1. Proposed BDC topology with dual-battery energy storage.

This bidirectional power switch is implemented via two metal-oxide-semiconductor field-effect

transistors (MOSFETs), pointing in opposite directions, in series connection. To explain the concept for the proposed converter, all the conduction statuses of the power devices involved in each operation mode are displayed in Table 2.1. Accordingly, the four operating modes are illustrated as follows to enhance understanding.

TABLE 2.1.
CONDUCTION STATUS OF DEVICES FOR DIFFERENT OPERATING MODES

Operating Modes	ON	OFF	Control Switch	Synchronous Rectifier (SR)
Low-voltage dual-source-powering mode (Accelerating, x_1=1, x_2=1)	S_{ES1}, S_{ES2}	S	Q_3, Q_4	Q_1, Q_2
High-voltage dc-bus energy-regenerating mode (Braking, x_1=1, x_2=1)	S_{ES1}, S_{ES2}	S	Q_1, Q_2	Q_3, Q_4
Low-voltage dual-source buck mode (ES1 to ES2, x_1=0, x_2=0)	S_{ES1}, S_{ES2}	Q_2, Q_3, Q_4	S	Q_1
Low-voltage dual-source boost mode (ES2 to ES1, x_1=0, x_2=0)	S_{ES1}, S_{ES2}	Q_1, Q_3, Q_4	Q_3	S
System shutdown	–	S_{ES1}, S_{ES2} Q_1, Q_2, Q_3, Q_4	–	–

2.1. Low-Voltage Dual-Source-Powering Mode

Fig. 2.2(a) depicts the circuit schematic and steady-state wave forms for the converter under the low-voltage dual-source-powering mode. Therein, the switch S is turned off, and the switches (SES1, SES2) are turned on, and the two low-voltage dual sources (VES1, VES2) are supplying the energy to the dc-bus and loads. In this mode, the low-side switches Q3 andQ4 are actively switching at a phase-shift angle of 180°, and the high-side switches Q1 and Q2 function as the synchronous rectifier (SR). Based on the typical waveforms shown in Fig. 2.2(b), when the duty ratio is larger than 50%, four circuit states are possible (Fig. 2.2). In the light of the on/off status of the active switches and the operating principle of the BDC in low-voltage dual-source-powering mode, the operation can be explained briefly as follows.

State 1 [t0 < t < t1]: During this state, the interval time is (1-Du)Tsw, switches Q1, Q3 are turned on, and switches Q2, Q4 are turned off. The voltage across L1 is the difference between the low-side voltage VES1 and the charge-pump voltage (VCB), and hence iL1 decreases linearly from the initial value. In addition, inductor L2 is charged by the energy source VES2,

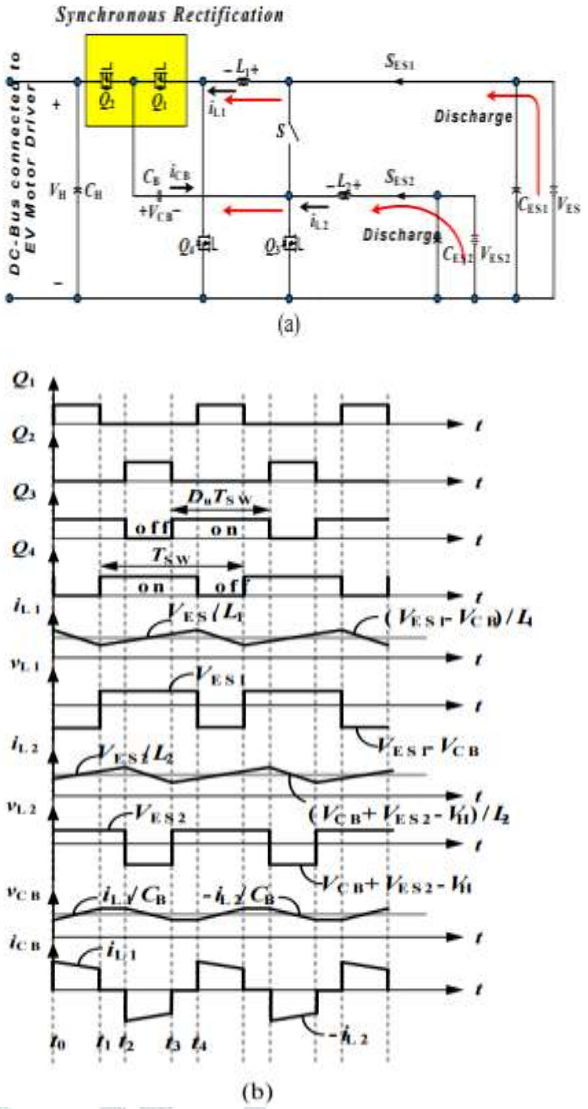

Fig. 2.2. Low-voltage dual-source-powering mode of the proposed BDC: (a) circuit schematic and (b) steady-state waveforms.

There by generating a linear increase in the inductor current. The voltages across inductors L1 and L2 can be denoted as

$$L_1 \frac{di_{L1}}{dt} = V_{ES2} - V_{CB} \qquad (1)$$

$$L_2 \frac{di_{L2}}{dt} = V_{ES2} \qquad (2)$$

State 2 [t1 < t < t2]: During this state, the interval time is (Du-0.5)Tsw; switches Q3 and Q4 are turned on; and switches Q1 and Q2 are turned

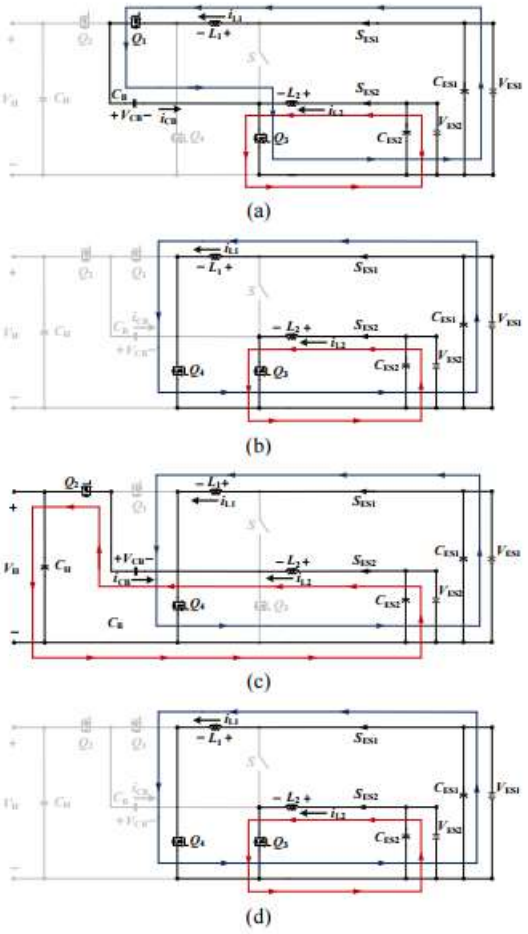

Fig. 2.3 Circuit states of the proposed BDC for the low-voltage dual-source-powering mode. (a) State 1. (b) State 2. (c) State 3. (d) State 4.

a) off. The low-side voltages VES1 and VES2 are located between inductors L1 and L2, respectively, thereby linearly increasing the inductor currents, and initiating energy to storage. The voltages across inductors L1 and L2 under state 2 can be denoted as

$$L_1 \frac{di_{L1}}{dt} = V_{ES1} \quad (3)$$

$$L_2 \frac{di_{L2}}{dt} = V_{ES2} \quad (4)$$

b) State 3 [t2 < t < t3]: During this state, the interval time is (1-Du)Tsw; switches Q1 and Q3 are turned on, whereas switches Q2 and Q4 are turned off. The voltages across inductors L1 and L2 can be denoted as

$$L_1 \frac{di_{L1}}{dt} = V_{ES1} \quad (5)$$

$$L_2 \frac{di_{L2}}{dt} = V_{CB} + V_{ES2} - V_H \quad (6)$$

c) State 4 [t3< t <t4]: During this state, the interval time is (Du-0.5)Tsw; switches Q3 and Q4 are turned on, and switches Q1 and Q2 are turned off. The voltages across inductors L1 and L2 can be denoted as

$$L_1 \frac{di_{L1}}{dt} = V_{ES1} \quad (7)$$

$$L_2 \frac{di_{L2}}{dt} = V_{ES2} \quad (8)$$

2.2. High-Voltage DC-Bus Energy-Regenerating Mode :

In this mode, the kinetic energy stored in the motor drive is fed back to the source during regenerative braking operation. The regenerative power can be much higher than what the battery can absorb. Consequently, the excess energy is used to charge the energy storage device. The circuit schematic and the steady-state waveforms of the BDC under the high-voltage dc bus energy-regenerating mode are illustrated in Fig.2.4.

Therein, the current in the inductors is controlled by the active switches Q1 and Q2, which have a phase-shift angle of 180° and thereby direct the flow away from the dc-bus and toward the dual energy storage devices; the switches Q3 and Q4 function as the SR to improve the conversion efficiency.

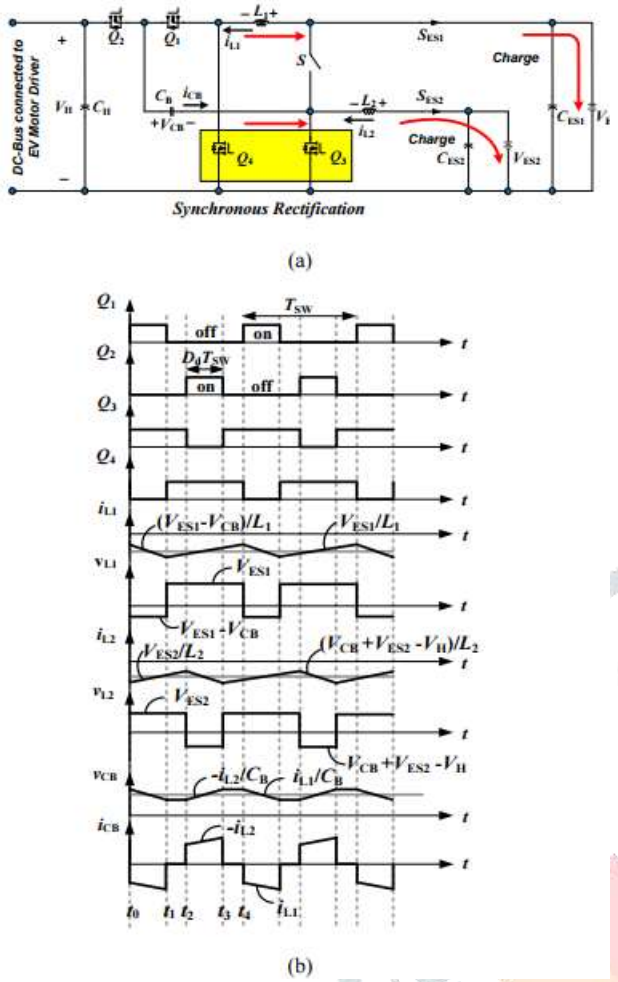

Fig.2.4. High-voltage dc-bus energy-regenerating mode of the proposed BDC: (a) circuit schematic and (b) steady-state waveforms.

On the basis of the steady-state waveforms shown in Fig. 2.4(b), when the duty ratio is below 50%, four different circuit states are possible, as shown in Fig. 2.5. In the light of the on-off status of the active switches and the operating principle of the BDC in high-voltage dc-bus energy-regenerating mode, the operation can be depicted briefly as follows.

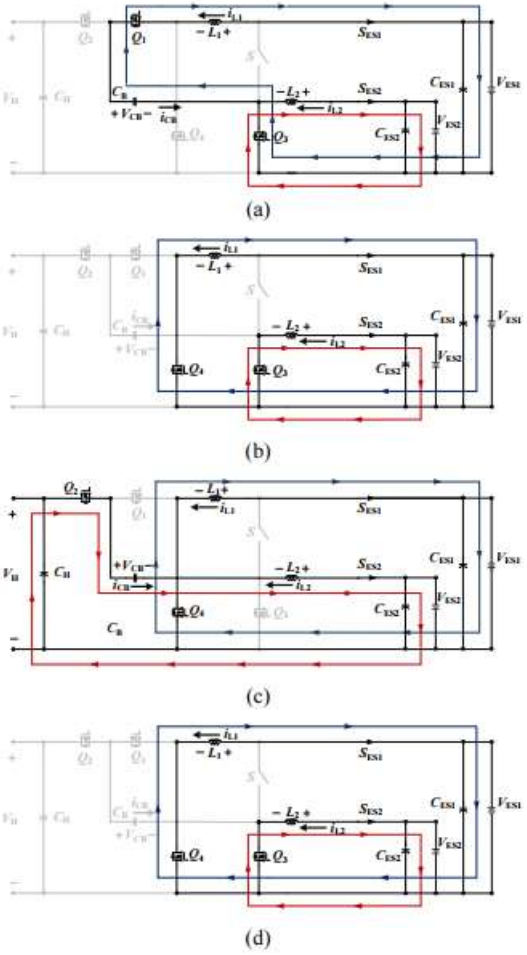

Fig. 2.5. Circuit states of the proposed BDC for the high-voltage dc-bus energy-regenerating mode. (a) State 1. (b) State 2. (c) State 3. (d) State 4.

a) State 1 [t0 < t < t1]: During this state, the interval time is Dd Tsw; switches Q1 and Q3 are turned on, and switches Q2 and Q4 are turned off. The voltage across L1 is the difference between the low-side voltage VES1 and the charge-pump voltage VCB; hence, the inductor current iL1 decreases linearly from the initial value. In addition, inductor L2 is charged by the energy source VES2, which also contributes to the linear increase in the inductor current. The voltages across inductors L1 and L2 can be denoted as

$$L_1 \frac{di_{L1}}{dt} = V_{ES1} - V_{CB} \qquad (9)$$

$$L_2 \frac{di_{L2}}{dt} = V_{ES2} \qquad (10)$$

b) State 2 [t1 < t < t2]: During this state, the interval time is (0.5-Dd)Tsw; switches Q3 and Q4 are turned on, and switches Q1and Q2 are turned off. The voltages across inductors L1 and L2 are the positive the

low-side voltages VES1 and VES2, respectively; hence, inductor currents iL1 and iL2 increase linearly. These voltages can be denoted as

$$L_1 \frac{di_{L1}}{dt} = V_{ES1} \quad (11)$$

$$L_2 \frac{di_{L2}}{dt} = V_{ES2} \quad (12)$$

c) State 3 [t2 < t < t3]: During this state, the interval time is DdTsw; switches Q1 and Q3 are turned off, and switches Q2 and Q4 are turned on. The voltage across L1 is the positive low-side voltage VES1 and hence iL1 increases linearly from the initial value. Moreover, the voltage across L2 is the difference of the high-side voltage VH, the charge-pump voltage VCB, and the low-side voltage VES2, and its level is negative. The voltages across inductors L1 and L2 can be denoted as

$$L_1 \frac{di_{L1}}{dt} = V_{ES1} \quad (13)$$

$$L_2 \frac{di_{L2}}{dt} = V_{ES2} + V_{CB} - V_H \quad (14)$$

d) State 4 [t3 < t < t4]: During this state, the interval time is (0.5-Dd)Tsw; switches Q3 and Q4 are turned on, and switches Q1 and Q2 are turned off. The voltages across inductors L1 and L2 can be denoted as

$$L_1 \frac{di_{L1}}{dt} = V_{ES1} \quad (15)$$

$$L_2 \frac{di_{L2}}{dt} = V_{ES2} \quad (16)$$

Remaining modes of operation were explained in [1].

3. FUZZY CONTROLLER:

The word Fuzzy means vagueness. Fuzziness occurs when the boundary of piece of information is not clear-cut. In 1965 Lotfi A. Zahed propounded the fuzzy set theory. Fuzzy set theory exhibits immense potential for effective solving of the uncertainty in the problem. Fuzzy set theory is an excellent mathematical tool to handle the uncertainty arising due to vagueness. Understanding human speech and recognizing handwritten characters are some common instances where fuzziness manifests.

Fuzzy set theory is an extension of classical set theory where elements have varying degrees of membership. Fuzzy logic uses the whole interval between 0 and 1 to describe human reasoning. In FLC the input variables are mapped by sets of membership functions and these are called as "FUZZY SETS".

Fuzzy set comprises from a membership function which could be defines by parameters. The value between 0 and 1 reveals a degree of membership to the fuzzy set. The process of converting the crisp input to a fuzzy value is called as "fuzzificaton." The output of the Fuzzier module is interfaced with the rules. The basic operation of FLC is constructed from fuzzy control rules utilizing the values of fuzzy sets in general for the error and the change of error and control action. Basic fuzzy module is shown in fig.5

The results are combined to give a crisp output controlling the output variable and this process is called as "DEFUZZIFICATION."

4.1 MATLAB CIRCUITS:

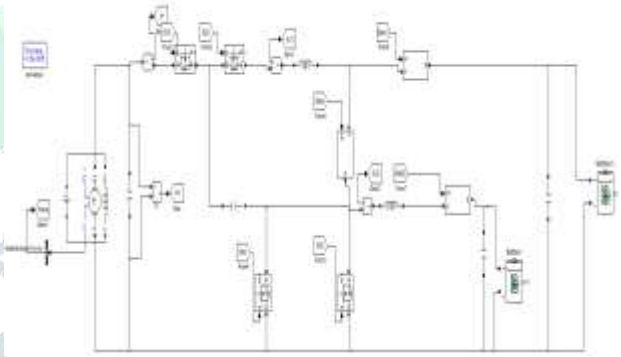

Fig4.1 Simulation Block Diagram

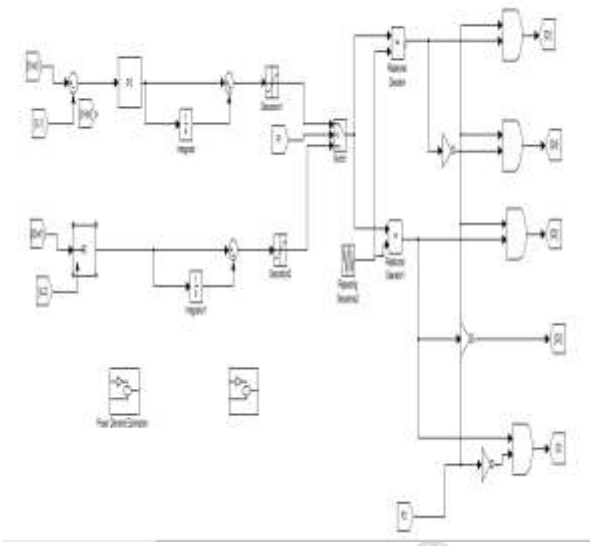

Fig4.2 Simulation Control Diagram

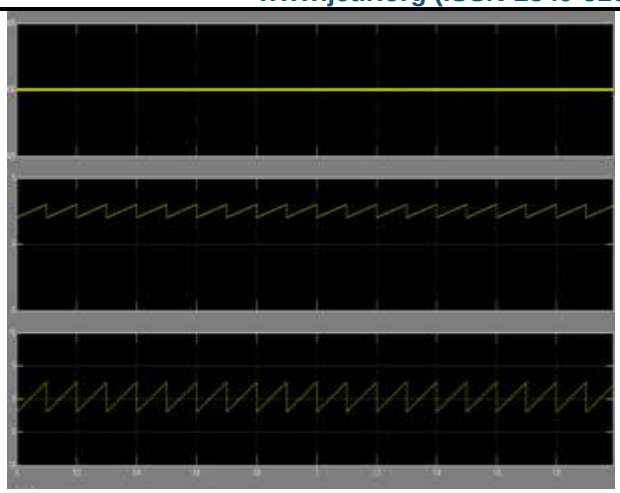

(b) output voltage and inductor currents.

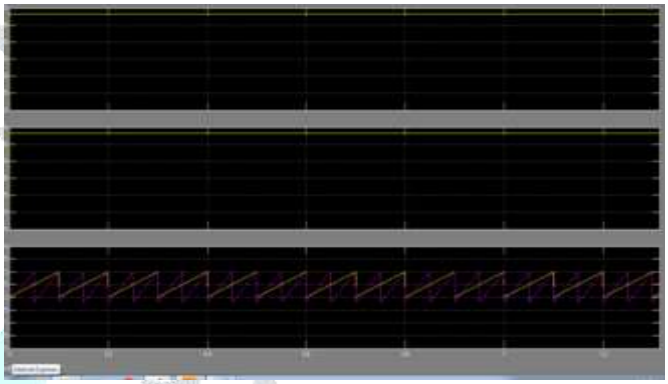

Fig. 4.4. Measured waveforms for high-voltage dc-bus energy-regenerating mode:.

4.2 WAVE FORMS:

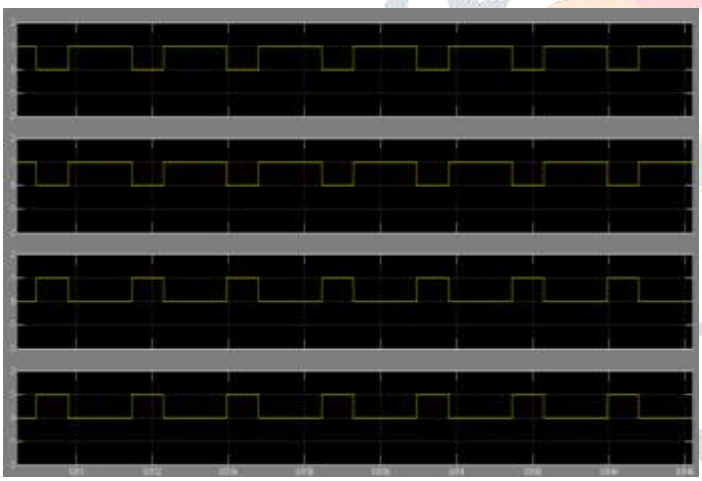

Fig. 4.3. Measured waveforms for low-voltage dual-source-powering mode:(a) gate signals

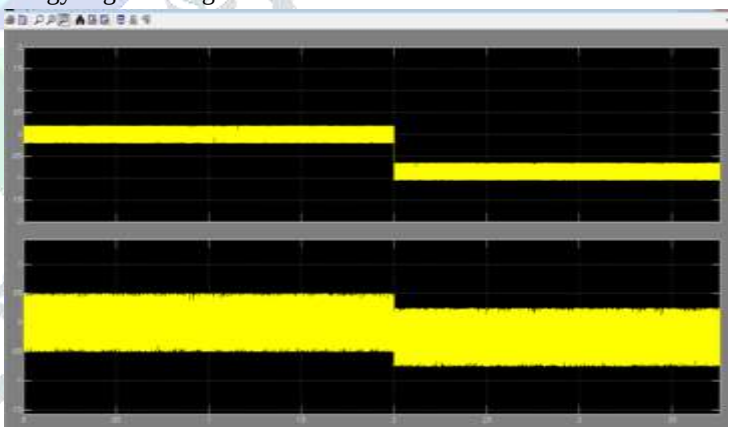

Fig.4.5. Waveforms of controlled current step change in the low-voltage dual-source-powering mode by simulation

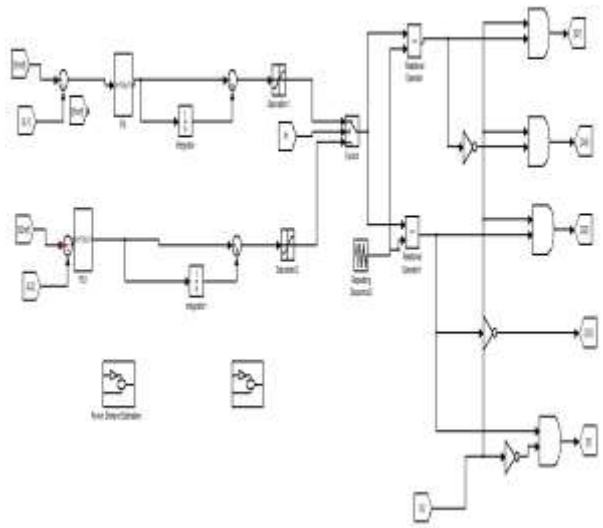

Fig4.6 Simulation of fuzzy logic Control Diagram

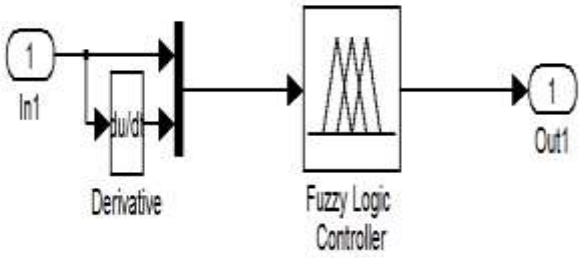

Fig4.7 fuzzy logic Controller

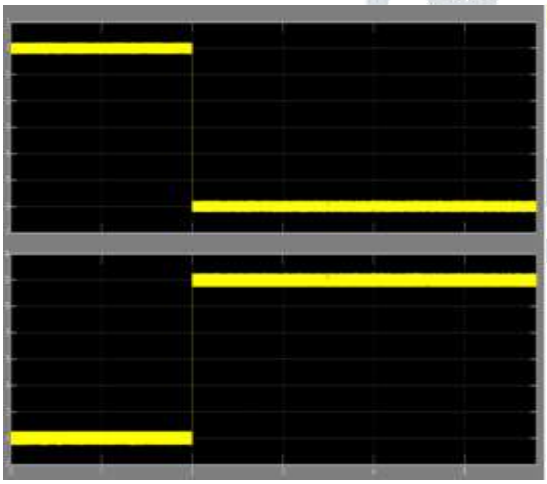

Fig. 4.8 Waveforms of controlled current step change in the low-voltage dual-source boost mode: by simulation;

Fig. 4.9 Waveforms of controlled current step change in the low-voltage dual- source buck mode: by simulation

CONCLUSION

A new BDC topology was presented to interface dual battery energy sources and high-voltage dc bus of different voltage levels. The circuit configuration, operation principles, analyses, and static voltage gains of the proposed BDC were discussed on the basis of different modes of power transfer. Simulation waveforms for a 1 kW prototype system highlighted the performance and feasibility of this proposed BDC topology. The highest conversion efficiencies were 97.25%, 95.32%, 95.76%, and 92.67% for the high-voltage dc-bus energy-regenerative buck mode, low-voltage dual-source-powering mode, low-voltage dual-source boost mode (ES2 to ES1), and low-voltage dual-source buck mode (ES1 to ES2), respectively. In this paper fuzzy logic controller is used to enhance the proposed topology. The results demonstrate that the proposed BDC can be successfully applied in FC/HEV systems to produce hybrid power architecture.

REFERENCES

[1] Ching-Ming Lai, Member, IEEE, Yu-Huei Cheng, Senior Member, IEEE, Ming-Hua Hsieh, and Yuan-Chih Lin" Development of a Bidirectional DC/DC Converter with Dual-Battery Energy Storage for Hybrid Electric Vehicle System" 2017 IEEE

[2] M. Ehsani, K. M. Rahman, and H. A. Toliyat, "Propulsion system design of electric and hybrid vehicles," IEEE Transactions on industrial electronics, vol. 44, no. 1, pp. 19-27, 1997.

[3] A. Emadi, K. Rajashekara, S. S. Williamson, and S. M. Lukic, "Topological overview of hybrid electric and fuel cell vehicular power system architectures and configurations," IEEE Transactions on Vehicular Technology, vol. 54, no. 3, pp. 763-770, 2005.

[4] A. Emadi, S. S. Williamson, and A. Khaligh, "Power electronics intensive solutions for advanced electric, hybrid electric, and fuel cell vehicular power systems," IEEE Transactions on Power Electronics, vol. 21, no. 3, pp. 567-577, 2006.

[5] P. Thounthong, V. Chunkag, P. Sethakul, B. Davat, and M. Hinaje, "Comparative study of fuel-cell vehicle hybridization with battery or supercapacitor storage device," IEEE transactions on vehicular technology, vol. 58, no. 8, pp. 3892-3904, 2009.

[6] C. C. Chan, A. Bouscayrol, and K. Chen, "Electric, hybrid, and fuel-cell vehicles: Architectures and modeling," IEEE transactions on vehicular technology, vol. 59, no. 2, pp. 589-598, 2010.

[7] A. Khaligh and Z. Li, "Battery, ultracapacitor, fuel cell, and hybrid energy storage systems for electric, hybrid electric, fuel cell, and plug-in hybrid electric vehicles: State of the art," IEEE transactions on Vehicular Technology, vol. 59, no. 6, pp. 2806-2814, 2010.

[8] K. Rajashekara, "Present status and future trends in electric vehicle propulsion technologies," IEEE Journal of Emerging and Selected Topics in Power Electronics, vol. 1, no. 1, pp. 3-10, 2013.

[9] C.-M. Lai, Y.-C. Lin, and D. Lee, "Study and implementation of a two-phase interleaved bidirectional DC/DC converter for vehicle and dc-microgrid systems," Energies, vol. 8, no. 9, pp. 9969-9991, 2015.

[10] C.-M. Lai, "Development of a novel bidirectional DC/DC converter topology with high voltage conversion ratio for electric vehicles and DC-microgrids," Energies, vol. 9, no. 6, p. 410, 2016.

[11] J. Moreno, M. E. Ortúzar, and J. W. Dixon, "Energy-management system for a hybrid electric vehicle, using ultracapacitors and neural networks," IEEE transactions on Industrial Electronics, vol. 53, no. 2, pp. 614-623, 2006.

[12] J. Bauman and M. Kazerani, "A comparative study of fuel-cell–battery, fuel-cell–ultracapacitor, and fuel-cell–battery–ultracapacitor vehicles," IEEE Transactions on Vehicular Technology, vol. 57, no. 2, pp. 760-769, 2008.

[13] M. Ehsani, Y. Gao, and A. Emadi, Modern electric, hybrid electric, and fuel cell vehicles: fundamentals, theory, and design. CRC press, 2009.

[14] Z. Haihua and A. M. Khambadkone, "Hybrid modulation for dual active bridge bi-directional converter with extended power range for ultracapacitor application," in Industry Applications Society Annual Meeting, 2008. IAS'08. IEEE, 2008, pp. 1-8: IEEE.

[15] H. Tao, J. L. Duarte, and M. A. Hendrix, "Three-port triple-half-bridge bidirectional converter with zero-voltage switching," IEEE transactions on power electronics, vol. 23, no. 2, pp. 782-792, 2008.

[16] T. Bhattacharya, V. S. Giri, K. Mathew, and L. Umanand, "Multiphase bidirectional flyback converter topology for hybrid electric vehicles," IEEE Transactions on Industrial Electronics, vol. 56, no. 1, pp. 78-84, 2009.

[17] H. Krishnaswami and N. Mohan, "Three-port series-resonant DC–DCconverter to interface renewable energy sources with bidirectional load and energy storage ports," IEEE Transactions on Power Electronics, vol. 24, no. 10, pp. 2289-2297, 2009.

[18] Y.-C. Liu and Y.-M. Chen, "A systematic approach to synthesizing multi-input DC–DC converters," IEEE Transactions on Power Electronics, vol. 24, no. 1, pp. 116-127, 2009.

[19] K. Gummi and M. Ferdowsi, "Double-input dc–dc power electronic converters for electric-drive vehicles—Topology exploration and synthesis using a single-pole triple-throw switch," IEEE Transactions on Industrial Electronics, vol. 57, no. 2, pp. 617-623, 2010.

[20] B. Zhao, Q. Song, and W. Liu, "Power characterization of isolated bidirectional dual-active-bridge DC–DC converter with dual-phase-shift control," IEEE Transactions on Power Electronics, vol. 27, no. 9, pp. 4172-4176, 2012.